


PRECLINICAL STUDY

Real-time laser speckle contrast imaging measurement during normothermic machine perfusion in pretransplant kidney assessment

Yitian Fang MD¹  | Lisanne van Ooijen MSc² | Gisela Ambagtsheer BSc¹ | Anton V. Nikolaev PhD³ | Marian C. Clahsen-van Groningen MD, PhD^{4,5} | Jenny Dankelman PhD² | Ron W. F. de Bruin PhD¹ | Robert C. Minnee MD, PhD¹

¹Department of Surgery, Division of HPB and Transplant Surgery, Transplant Institute, Erasmus Medical Center, Rotterdam, the Netherlands

²Department of Biomechanical Engineering, Delft University of Technology, Delft, the Netherlands

³Department of Cardiology, Erasmus Medical Center, Rotterdam, the Netherlands

⁴Department of Pathology and Clinical Bioinformatics, Erasmus Medical Center, Rotterdam, the Netherlands

⁵Institute of Experimental and Systems Biology, RWTH Aachen University, Aachen, Germany

Correspondence

Robert C. Minnee, MD, PhD, Department of Surgery, Division of HPB and Transplant Surgery, Transplant Institute, Erasmus Medical Center, Rotterdam, the Netherlands.
Email: r.minnee@erasmusmc.nl

Abstract

Objectives: Normothermic machine perfusion (NMP) provides a platform for pretransplant kidney quality assessment that is essential for the use of marginal donor kidneys. Laser speckle contrast imaging (LSCI) presents distinct advantages as a real-time and noncontact imaging technique for measuring microcirculation. In this study, we aimed to assess the value of LSCI in visualizing renal cortical perfusion and investigate the additional value of dual-side LSCI measurements compared to single aspect measurement during NMP.

Methods: Porcine kidneys were obtained from a slaughterhouse and then underwent NMP. LSCI was used to measure one-sided cortical perfusion in the first 100 min of NMP. Thereafter, the inferior renal artery branch was occluded to induce partial ischemia and LSCI measurements on both ventral and dorsal sides were performed.

Results: LSCI fluxes correlated linearly with the renal blood flow ($R^2 = 0.90$, $p < 0.001$). After renal artery branch occlusion, absence of renal cortical perfusion could be visualized and semiquantified by LSCI. The overall ischemic area percentage of the ventral and dorsal sides was comparable (median interquartile range [IQR], 38 [24–43]% vs. 29 [17–46]%, $p = 0.43$), but heterogenous patterns between the two aspects were observed. There was a significant difference in oxygen consumption (mean \pm standard deviation [SD], 2.57 ± 0.63 vs. 1.83 ± 0.49 mL O_2 /min/100 g, $p < 0.001$), urine output (median [IQR], 1.3 [1.1–1.7] vs. 0.8 [0.6–1.3] mL/min, $p < 0.05$), lactate dehydrogenase (mean \pm SD, 768 ± 370 vs. 905 ± 401 U/L, $p < 0.05$) and AST (mean \pm SD, 352 ± 285 vs. 462 ± 383 U/L, $p < 0.01$) before and after renal artery occlusion, while no significant difference was found in creatinine clearance, fractional excretion of sodium, total sodium reabsorption and histological damage.

Conclusions: LSCI fluxes correlated linearly with renal blood flow during NMP. Renal cortical microcirculation and absent perfusion can be visualized and semiquantified by LSCI. It provides a relative understanding of perfusion levels, allowing for a qualitative comparison between regions in the kidney. Dual-side LSCI measurements are of added value compared to single aspect measurement and renal function markers.

KEYWORDS

kidney quality assessment, laser speckle contrast imaging, normothermic machine perfusion, renal cortical microcirculation

INTRODUCTION

Kidney transplantation is the optimal treatment for patients with end stage renal disease.¹ However, due to the shortage of organs, expanded criteria donor (ECD) and donation after circulatory death (DCD) kidneys are increasingly being used to enlarge the donor pool.^{2,3} Unfortunately, a significant proportion of ECD and DCD kidneys are associated with impaired function and graft failure.^{2,4} To improve clinical outcomes after transplantation, normothermic machine perfusion (NMP) has emerged as a viable platform for graft quality assessment by simulating the body's environment, which is essential for the use of these marginal donor kidneys.⁵ Using imaging techniques during NMP is a potentially relevant, but poorly explored field to assess graft quality. Laser speckle contrast imaging (LSCI), as a real-time, noncontact, full-field imaging technique with a large field of view,⁶ has gained interest as an imaging technique for evaluating microvascular circulation of various tissues, such as retina, cerebrum, skin and liver.^{7–11} Despite extensive research on LSCI, few studies have explored its potential as kidney quality assessment tool. The only study that has used LSCI to measure the kidney during NMP, conducted by Heeman et al.¹² showed that one-sided measurement can assess cortical microcirculation and detect perfusion deficits. However, it is unknown whether there is heterogeneity of microcirculation between the ventral and dorsal aspects. Therefore, in this study, we aimed to investigate the value of LSCI in the assessment of renal cortical perfusion and determine the potential added value of measuring perfusion across the entire kidney surface. Additionally, we explored the added value of LSCI compared to standard clinical flow and functional parameters during NMP.

MATERIALS AND METHODS

Animal model

Porcine kidneys ($n = 10$) from the slaughterhouse were used. Kidneys were obtained from female landrace pigs weighing 100–120 kg at a local slaughterhouse. These kidneys were procured to mimic the DCD donor procedure.¹³ At the same time, two liters of blood from the same pig were collected in a bucket containing 25,000 IU of heparin (LEO Pharma A/S). After cannulating the renal artery with a 5-mm straight cannula (Organ Recovery Systems), kidneys were flushed with 4°C Ringer's lactate (Baxter BV). Next, the kidneys were placed inside the LifePort Kidney Transporter 1.0

(Organ Recovery Systems) and perfused at 30 mmHg with 4°C Belzer UW machine perfusion solution (Belzer MPS, Bridge to Life Ltd.) until NMP. The estimated time from kidney procurement to NMP ranged from 24 to 36 h. As we used the standard organ preservation method in the Netherlands, no significant impact was anticipated on our research outcomes. Warm ischemia time (WIT) was calculated from the end of blood collection until the beginning of cold solution flushing. As the kidneys were from pigs slaughtered for meat consumption, no approval from the animal ethics committee was required.

Study design

The study consists of two distinct parts: reperfusion measurement and dual-side measurements. Before NMP, LSCI was used to obtain baseline fluxes of the kidneys without perfusion. The kidneys were then subjected to NMP, and LSCI measurement was performed on ventral side only at 10-min intervals for 100 min. The kidneys were continuously perfused until the renal blood flow stabilized, followed by dual-side measurements. To achieve this, the ventral side measurement was performed while the kidney was placed in the reservoir with the ventral side facing upwards. Subsequently, the dorsal side measurement was performed after manually turning over the kidney. After measuring both sides, the inferior branch of the renal artery was occluded by vascular clamps or ligation to induce renal infarction. The dual-side measurements were then repeated one time, when the hemodynamics regained stability.

NMP

After the cold preservation period, kidneys were flushed with 200 mL cold Ringer's lactate (Baxter) before ex vivo NMP. The NMP system consists of a custom-made organ chamber, a centrifugal pump head (BPX-80 Bio-Pump™ Plus; Medtronic) equipped with pump drive (BVP-BP; Harvard Apparatus), an oxygenator with heat exchanger (Hilite 1000; Medos) and a thermocirculator (E100). The flow probe (73-4755; Harvard Apparatus) was positioned in-line and the pressure transducer (APT300, Harvard Apparatus) was directly connected to the renal artery cannula (Organ Recovery Systems). The set-up was controlled by a commercially available electronic controller (PLUGSYS Servo Controller for Perfusion, Harvard Apparatus) which enables both flow and pressure-directed perfusion. The kidneys were

perfused with autologous leukocyte depleted (leukocyte filter BioR 02 plus BS PF, Fresenius Kabi, Zeist, the Netherlands) blood-based solution (Supporting Information: Table S1)¹³ at 37°C with a controlled pressure of 70 mmHg. During NMP, carbogen (95% O₂ and 5% CO₂) was supplied via the oxygenator at a flow rate of 500 mL/min. Each kidney was weighed both before and after NMP.

LSCI measurement

A commercially available LSCI system with a laser wavelength of 785 nm (MoorO₂Flo; Moor Instruments Ltd.) was placed above the kidney (Figure 1). The exposure time was 20 ms and spatial resolution was 3.9 microns per pixel. The working distance between the camera and the kidney was 20 cm to ensure the kidney was in the field of view. To perform LSCI, an opaque cover was placed over the setup to block all ambient light. To test the definition of LSCI, the images of four kidneys were processed in low resolution mode (116 × 150 pixels), and the remaining

six kidneys were in high resolution mode (576 × 748 pixels). The processing algorithm was the same in each case and the only difference is the pixel resolution of the resulting images. Image frames were recorded at the rate of 20 Hz. Each measurement lasted for 10 s and 201 frames were recorded in total. The whole kidney was chosen as the region of interest (ROI) for further analyses. The measure mode is spatial with a kernel size of 5 × 5 pixels to calculate the speckle contrast K using the equation:

$$K = \frac{\sigma}{\langle I \rangle}, \quad (1)$$

where σ is the standard deviation (SD) of the intensity I , and $\langle I \rangle$ is the mean intensity. In this mode, the basic formula for LSCI measurement of renal perfusion (Flux) is

$$\text{Flux} \propto \left(\frac{\langle I \rangle}{\sigma} \right)^2, \quad (2)$$

and measured in perfusion unit (PU).

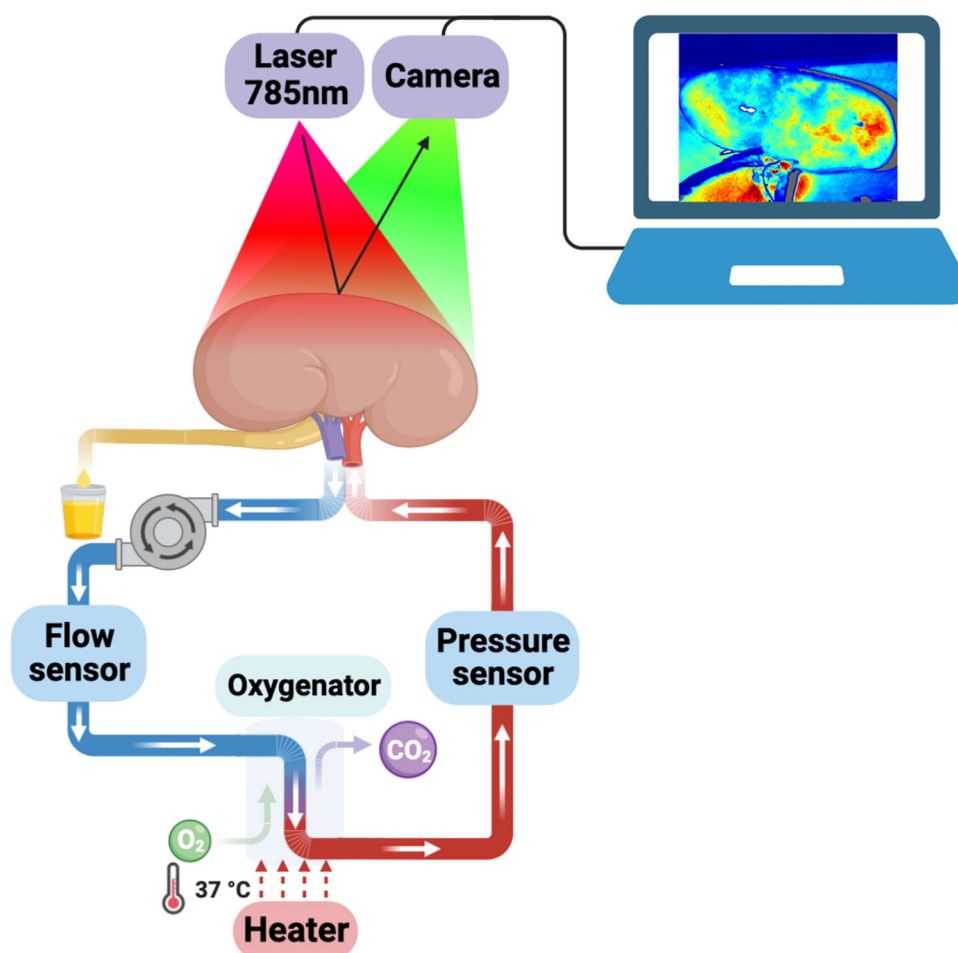


FIGURE 1 Schematic overview of the combined normothermic machine perfusion (NMP) and laser speckle contrast imaging (LSCI) setup.

Renal function and injury assessment

Renal blood flow was recorded every 10 min. The percentage of blood flow decline was calculated using the formula $\frac{V_{before} - V_{after}}{V_{before}} \times 100\%$, where V_{before} is the blood flow before clamping the renal artery, and V_{after} is the blood flow after clamping the renal artery. The ratio of ischemic area was calculated using the formula $\frac{N_{all} - N_{ischemia}}{N_{all}} \times 100\%$, where N_{all} represents the number of pixels of the whole ROI, and $N_{ischemia}$ represents the number of pixels within the ischemic area. Perfusate samples from renal artery and vein, as well as urine samples, were taken before and after renal artery occlusion. Blood gas analyses enabled the calculation of oxygen consumption (VO_2). Perfusate and urine concentrations of lactate dehydrogenase (LDH), aspartate aminotransferase (AST), creatinine and sodium were determined in the hospital biochemistry laboratory using routine clinical assays. The concentrations of creatinine and sodium enabled the calculation of creatinine clearance (CrCl), fractional excretion of sodium (FENa) and total sodium reabsorption (TNa), of which the equations^{13,14} are presented in Supporting Information: Table S2.

Cortical tissues from both nonischemic and ischemic areas were collected after NMP and fixed in 4% buffered paraformaldehyde for 48 h. The tissue samples were then embedded in paraffin and cut into 4 μ m sections. Using periodic acid-Schiff (PAS) staining, renal tubular necrosis was evaluated and scored on a semiquantitative scale of 0–3 (0-no changes, 1-mild, 2-moderate, 3-severe changes) by an experienced renal pathologist (MCvG) blinded to the study. The tubular injury score was based on the degree of brush border loss, tubular dilatation, epithelial vacuolation, thinning and sloughing, and luminal debris/casts.

Statistical analysis

Continuous variables were tested for normality using Shapiro–Wilk test and reported as mean \pm SD if

normally distributed or median with interquartile range (IQR) in the case of non-normal distribution. To compare the LSCI flux, renal function and tubular injury before and after arterial clamping, continuous variables were compared using the paired *t*-test or Wilcoxon signed-rank test depending on the normality. The raw LSCI data were processed using MATLAB (MathWorks, Inc.). Statistical analyses were performed using SPSS version 26 (SPSS Inc.). The graphs were plotted using GraphPad Prism 9.3.1 (GraphPad Software Inc.). A $p \leq 0.05$ was considered statistically significant.

RESULTS

All kidneys were included in the analyses. The WIT of the kidneys was 38.4 ± 8.5 min. The weight of the kidneys was 283 ± 45 g before NMP and 318 ± 53 g after NMP.

Reperfusion measurement

The representative LSCI patterns from low resolution and high resolution modes were shown in Figure 2, and the flux measurements for each kidney at representative time points were displayed in Supporting Information: Table S3. During the first 100 min of NMP, an increase of renal cortical perfusion could be clearly visualized through LSCI (Figure 3A). The mean value of each measurement was used to explore the relevance between the renal blood flow and LSCI flux. With the increase of blood flow, LSCI fluxes also increased correspondingly, from the baseline of 63 ± 44 PU to 797 ± 271 PU (Figure 3B). The LSCI flux correlated linearly with the renal blood flow ($R^2 = 0.90$, $p < 0.001$, Figure 3C).

Dual-side LSCI measurement

All kidneys were adequately perfused without macroscopic ischemic lesions based on a visual inspection of

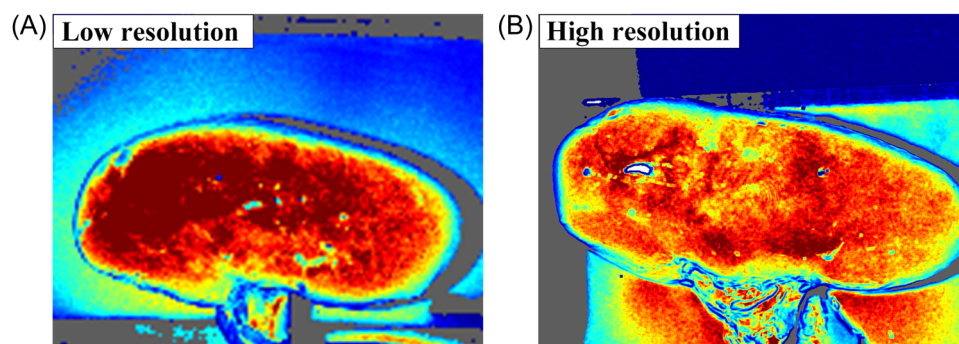


FIGURE 2 Representative LSCI patterns of the kidneys from (A) low resolution mode and (B) high resolution mode during NMP. LSCI, laser speckle contrast imaging; NMP, normothermic machine perfusion.

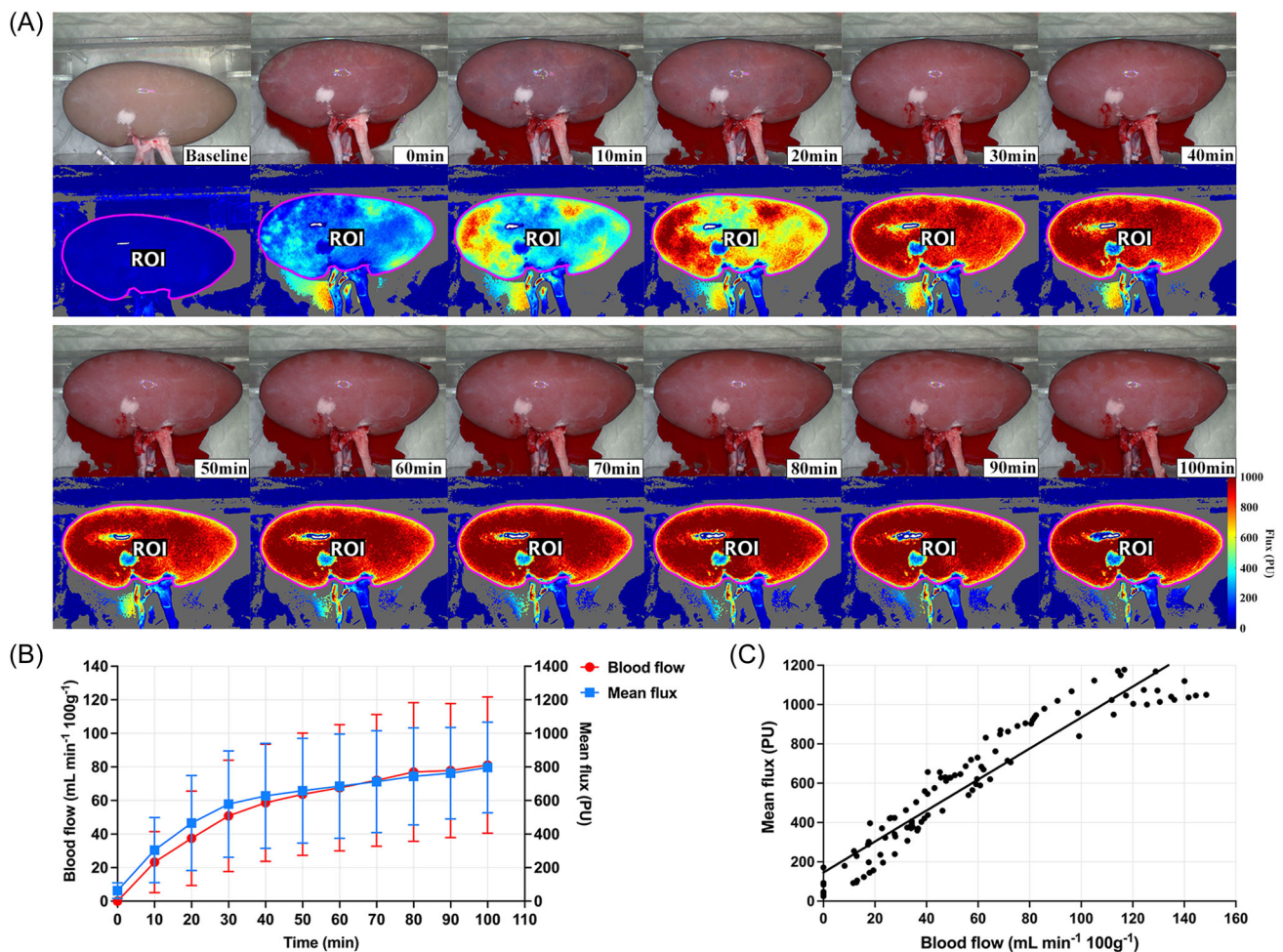


FIGURE 3 (A) Macroscopic appearances (above) and the corresponding LSCI patterns (below) of one kidney during the first 100 min of NMP. (B) Renal blood flow and the LSCI flux during the first 100 min of NMP. (C) Linear regression analysis on LSCI flux versus renal blood flow during the first 100 min of NMP ($R^2 = 0.90$, $p < 0.001$). LSCI, laser speckle contrast imaging; NMP, normothermic machine perfusion; ROI, region of interest.

homogeneously pink outer surface. The LSCI fluxes were 885 ± 234 PU on the ventral side and 931 ± 295 PU on the dorsal side. As shown in Figure 4, a decline of blood flow was observed in all kidneys by 14%–48% after clamping the renal artery branch. Part of the previously well-perfused region was replaced by ischemic lesions and the infarct border was clearly identified by LSCI. In eight out of ten kidneys, ischemic lesions could be seen on both sides after the artery branch occlusion (Figure 5A), with a percentage of the surface ranging from 23% to 49% on the ventral side and 16% to 58% on the dorsal side. However, in the remaining two kidneys, an ischemic lesion could be observed on only one side, with 46% of the ventral side and 58% of the dorsal side affected (Figure 5B), respectively. Compared to the LSCI measurement before clamping, the fluxes on both sides were significantly decreased after artery branch occlusion (ventral side: median [IQR], 912 [657–1082] vs. 484 [420–740] PU, Wilcoxon matched-pairs signed rank, $p < 0.01$; dorsal side: median [IQR], 943 [741–1212] vs.

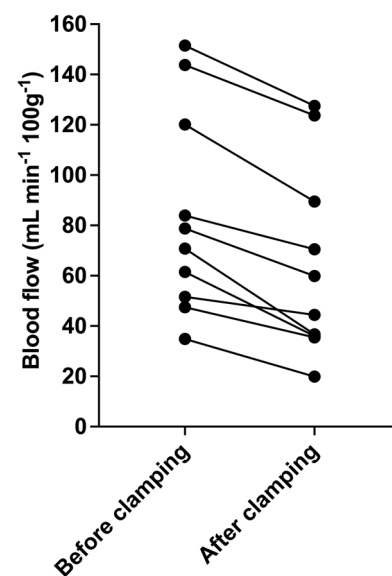


FIGURE 4 Renal blood flow changes before and after the renal artery branch occlusion.

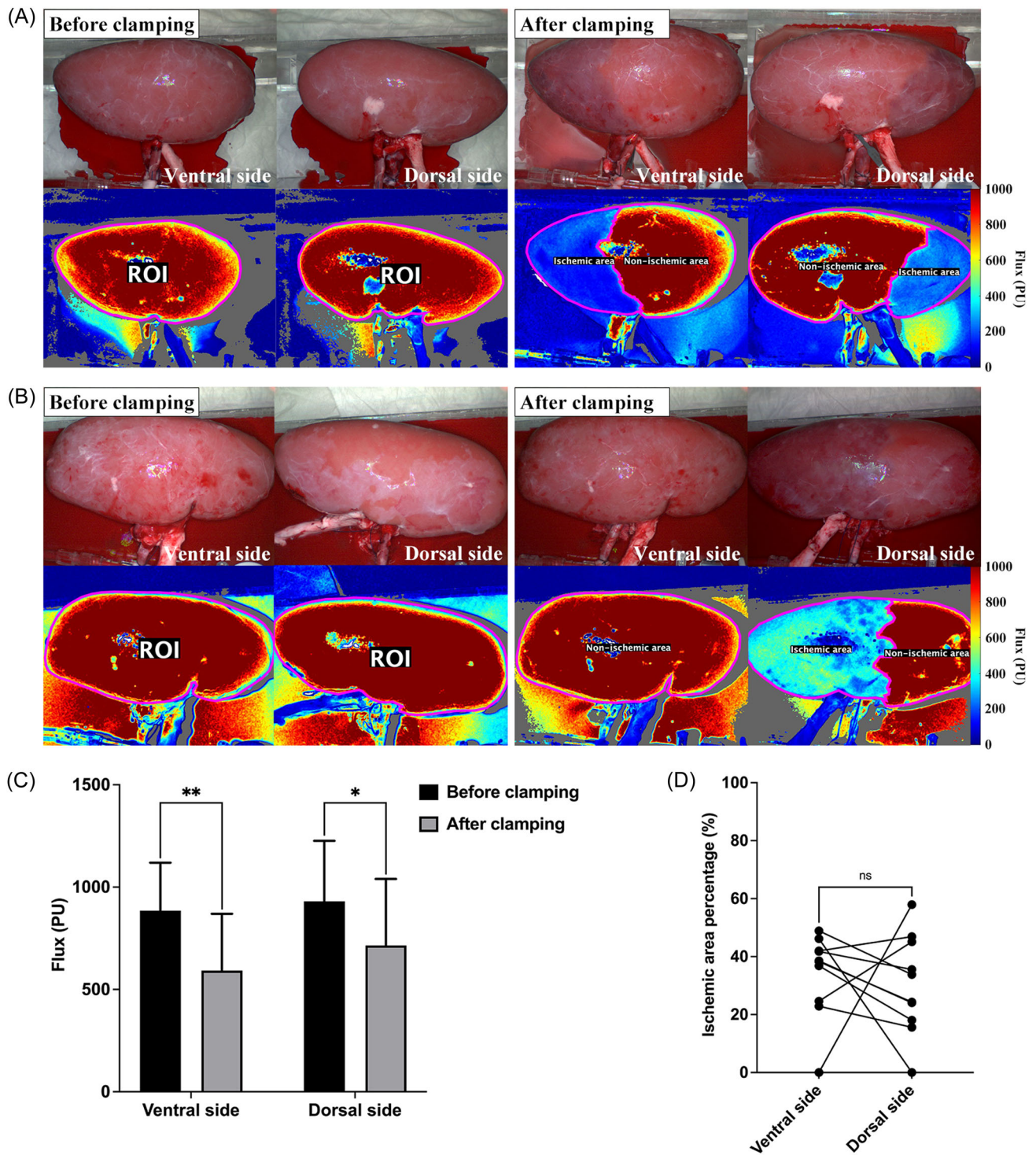


FIGURE 5 Representative macroscopic appearances and LSCI patterns of renal cortical perfusion in two different situations after the renal artery branch occlusion during NMP: (A) Ischemic lesions could be seen on both ventral and dorsal sides after artery branch occlusion, with ischemia in 39% and 24% of the whole area, respectively; (B) Ischemic lesions could be observed on only one side after artery branch occlusion, inducing ischemia in 58% of the dorsal area. (C) LSCI flux of the kidneys on the ventral and dorsal sides before and after the renal artery branch occlusion during NMP. (D) Ischemic area percentage of all kidneys on the ventral and dorsal sides. Wilcoxon matched-pairs signed rank. * $p < 0.05$, ** $p < 0.01$, *** $p < 0.001$. LSCI, laser speckle contrast imaging; NMP, normothermic machine perfusion; ROI, region of interest.

600 [408–1057] PU, Wilcoxon matched-pairs signed rank, $p < 0.01$, Figure 5C). The ischemic area ratio between the ventral and dorsal sides was comparable (median [IQR], 38 [24–43]% vs. 29 [17–46]%, Wilcoxon

matched-pairs signed rank, $p = 0.43$, Figure 5D). The comparison of histograms before and after artery occlusion provided insight into the changes in renal cortical perfusion (Supporting Information: Figure S1).

Renal function

As a surrogate marker for the glomerular filtration rate, CrCl tended to decrease after renal artery occlusion (median [IQR], 0.94 [0.68–1.11] vs. 0.61 [0.35–0.94] mL/min/100 g, Wilcoxon matched-pairs signed rank, $p = 0.06$), but the difference was not statistically significant (Figure 6A). To evaluate tubular transport function, FENa was calculated. Kidneys showed comparable FENa before and after occlusion during NMP (median [IQR], 60.2 [27.0–83.4]% vs. 51.9 [22.8–77.9]%, Wilcoxon matched-pairs signed rank, $p = 0.32$, Figure 6B). Although VO_2 significantly decreased after clamping the artery (2.57 ± 0.63 vs. 1.83 ± 0.49 mL O_2 /min/100 g, paired t -test, $p < 0.001$, Figure 6C), the capability of reabsorbing the sodium was similar before and after occlusion (median [IQR], 47.75 [10.86–126.47] vs. 37.21 [11.76–106.06] mmol/min/100 g, Wilcoxon matched-pairs signed rank, $p = 0.63$, Figure 6D). Before occlusion, kidneys showed a significantly higher urine output than

after occlusion (median [IQR], 1.3 [1.1–1.7] vs. 0.80 [0.6–1.3] mL/min, Wilcoxon matched-pairs signed rank, $p < 0.05$, Figure 6E).

Renal injury measurement

To evaluate renal injury, LDH and AST concentrations in perfusate were measured. LDH concentrations became significantly higher after occlusion (768 ± 370 vs. 905 ± 401 U/L, paired t -test, $p < 0.05$, Figure 6F). Similarly, AST concentrations were also higher after occlusion (352 ± 285 vs. 462 ± 383 U/L, paired t -test, $p < 0.01$, Figure 6G). Moreover, PAS-stained renal sections were scored on a scale from 1 to 3 based on acute tubular necrosis (ATN). In both nonischemic and ischemic tissue, biopsies showed moderate ATN with proximal tubule dilation and absence of brush border (Figure 7A), with no difference between the groups (2.45 ± 0.50 vs. 2.50 ± 0.47 , paired t -test, $p = 0.34$, Figure 7B).

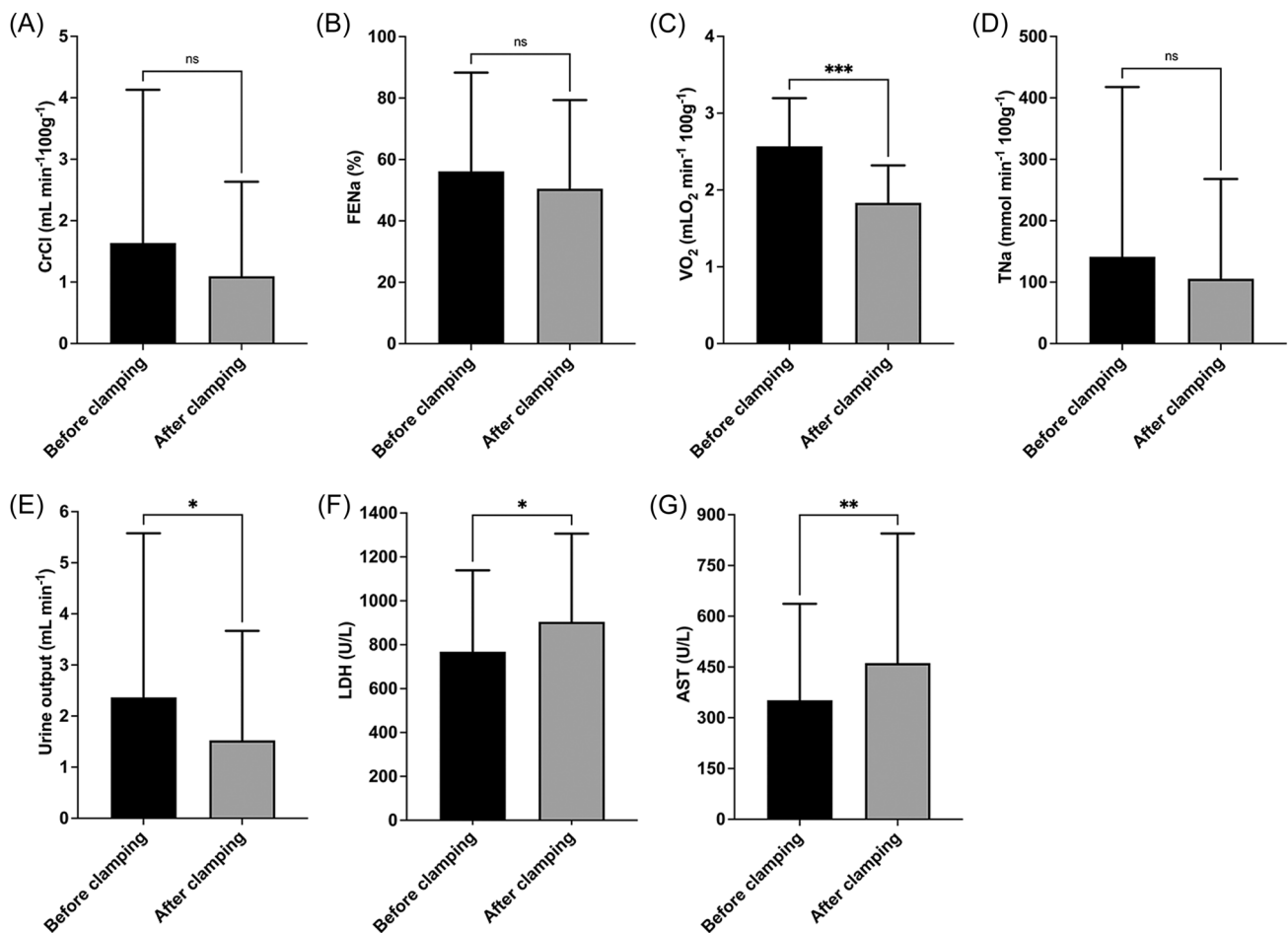


FIGURE 6 Renal function and injury makers before and after inferior renal artery branch occlusion during NMP. (A) creatinine clearance (CrCl, mL/min/100 g); (B) fractional excretion of sodium (FENa, %); (C) oxygen consumption (VO_2 , mL O_2 /min/100 g); (D) total sodium reabsorption (TNa, mmol/min/100 g); (E) urine output (mL/min); (F) lactate dehydrogenase (LDH, U/L) and (G) aspartate aminotransferase (AST, U/L). Data presented as mean \pm SD. (A), (B), (D), (E), Wilcoxon matched-pairs signed rank, and (C), (F), (G), paired t -test. * $p < 0.05$, ** $p < 0.01$, *** $p < 0.001$. LSCI, laser speckle contrast imaging; NMP, normothermic machine perfusion; SD, standard deviation.

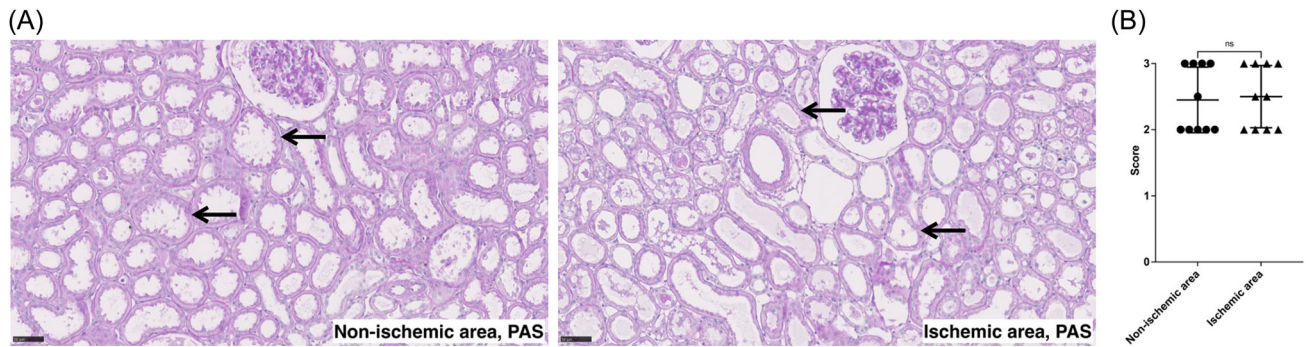


FIGURE 7 (A) Histomorphology of both nonischemic and ischemic areas showed moderate severity of acute tubular injury, tubular dilation and proximal tubule brush border loss. (B) Tissues were assessed based on acute tubular necrosis using paired *t*-test (ranging from mild to severe: 1–3). Black arrows indicate dilated proximal tubules with brush border loss. PAS, periodic acid-Schiff.

DISCUSSION

In this study, we conducted LSCI measurements in human-sized porcine kidneys during NMP. The reperfusion experiment demonstrated a strong linear correlation between LSCI fluxes and renal blood flow. Furthermore, by conducting dual-side measurements, we were able to visualize and semiquantify the renal cortical microcirculation and perfusion decline using LSCI. Dual-side LSCI measurements provided more comprehensive information than single-sided measurement.

LSCI relies on the blurring effect of the speckle phenomenon, which occurs when a scattering object is illuminated by coherent laser light. The interference pattern formed by the backscattered light creates a speckle pattern.^{6,15,16} In LSCI, this blurring effect is used to visualize blood flow by tracking the motion of red blood cells. However, LSCI only provides relative measurements of blood flow rather than absolute values.^{16,17} A larger value of perfusion units corresponds to more perfusion, which means more movement of red blood cells. Despite similar macroscopic appearances, LSCI revealed heterogeneities in microcirculation across individual kidneys and over time. Our study found that the LSCI flux correlated linearly with the renal blood flow when the distance between the kidney and camera was fixed, which is consistent with findings by Heeman et al.¹² With approximately 85% nephrons as cortical nephrons,¹⁸ most of the ultrafiltration and electrolyte reabsorption occur in the renal cortex. Therefore renal cortical perfusion likely provides more information on kidney viability and function than general blood flow.

During the dual-side measurements, we occluded the inferior renal artery branch to induce renal infarction, simulating arterial stenosis and thrombosis. Compared to the macroscopic appearance, LSCI enabled a more sensitive identification and semiquantification of the ischemic lesion. Although no statistical difference was found in the ischemic areas between the ventral and dorsal sides, none of the kidneys displayed the same patterns of infarction on both aspects, and two kidneys

showed renal infarction on one aspect only. This indicates the heterogeneities in vascular anatomy and intrarenal blood distribution between the ventral and dorsal sides. Considering the more complex variation in renal artery anatomy,¹⁹ this heterogeneity of segmental blood supply in human kidneys could be even greater. As a rapid and noninvasive imaging technique, dual-side LSCI measurements provide more information on cortical perfusion and deficiency than single aspect measurement without extending the time of organ exposure.

Currently, Doppler ultrasound is used as the standard of care to examine renal blood flow. It requires physical contact between the probe and the object being measured, which increases risk of contamination. In the preclinical phase, Schutter et al.²⁰ used magnetic resonance imaging (MRI) to visualize the perfusate distribution in renal cortex and medulla during NMP. However, the use of MRI during NMP requires a large volume of blood-based perfusate and complicated procedures, which limits its practicality. Compared to ultrasound and MRI, LSCI provides a simple, valuable alternative for real-time cortical perfusion assessment. Additionally, it is promising to apply LSCI to intraoperative diagnosis of anastomotic stenosis which typically occurs shortly after kidney reperfusion during transplantation and may lead to graft impairment and failure.^{21,22}

As the LSCI patterns in both low resolution and high resolution modes can effectively detect microcirculation changes, the choice of resolution mode depends on specific research objectives and the desired level of details. Low resolution mode offers faster image processing, which can be advantageous when analyzing a large number of images. However, the main drawback of low resolution mode is the reduction in image details, leading to the loss of nuances in the speckle patterns. High resolution mode captures more crucial details, allowing for more precise analysis of microcirculation. The higher pixel density in high resolution images leads to sharper and more visually informative images, helping researchers and clinicians identify subtle microcirculatory

changes. However, processing high resolution images requires more computational resources and time.

Besides LSCI measurements, renal function and injury were also measured. Urine output dropped significantly after clamping the renal artery branch, as did the oxygen consumption. However, no significant difference was found in CrCl, FENa and TNa. Renal injury markers, LDH and AST were significantly elevated after renal artery occlusion in the perfusate. However, histology showed no significant differences between the ischemic and nonischemic areas. The reason for this may be that the ischemia time was not long enough to induce renal injury that can be identified histologically. It is currently unclear whether occluding a branch of the renal artery would trigger a compensatory increase in blood flow in the remaining sections of the kidney. However, relying solely on renal function and injury markers may lead to the oversight of regional perfusion deficiencies.

Our study has several limitations to be addressed. Firstly, the use of slaughterhouse kidneys might result in higher interindividual variability in kidney viability and extent of renal injury, which could have interfered with our outcome measurements. Secondly, although LSCI is a powerful technique for recording blood perfusion, the physics of the scattering process is complex and unable to measure absolute flow, making it difficult to statistically compare perfusion between individuals. Thirdly, the measurement depth of LSCI is limited to 0.9 mm,²³ which restricts its ability to measure deeper areas of the kidney. Lastly, further studies using a transplant model should be conducted to validate our findings.

CONCLUSION

LSCI is a promising real-time imaging technique for assessing renal cortical perfusion during NMP. Our results indicate that LSCI fluxes have a strong linear correlation with renal blood flow, and LSCI can be used to visualize and semiquantify renal cortical microcirculation and perfusion deficiency. Moreover, dual-side LSCI measurements provides complementary information compared to single aspect measurements, which is not reflected by standard renal function and morphology assessment. Therefore, we recommend dual-side LSCI measurements as an additional kidney perfusion assessment tool during NMP, which is crucial for evaluating organ viability and improving clinical outcomes after transplantation.

CONFLICT OF INTEREST STATEMENT

The authors declare no conflict of interest.

ORCID

Yitian Fang  <http://orcid.org/0000-0002-5523-9794>

REFERENCES

1. Tonelli M, Wiebe N, Knoll G, Bello A, Browne S, Jadhav D, et al. Systematic review: kidney transplantation compared with dialysis in clinically relevant outcomes. *Am J Transplant (AJT)*. 2011;11(10):2093–109.
2. Port FK, Bragg-Gresham JL, Metzger RA, Dykstra DM, Gillespie BW, Young EW, et al. Donor characteristics associated with reduced graft survival: an approach to expanding the pool of kidney donors. *Transplantation*. 2002;74(9):1281–6.
3. Lomero M, Gardiner D, Coll E, Haase-Kromwijk B, Procaccio F, Immer F, et al. Donation after circulatory death today: an updated overview of the European landscape. *Transpl Int*. 2020;33(1):76–88.
4. Hamed MO, Chen Y, Pasea L, Watson CJ, Torpey N, Bradley JA, et al. Early graft loss after kidney transplantation: risk factors and consequences. *Am J Transplant (AJT)*. 2015;15(6):1632–43.
5. Hosgood SA, Thompson E, Moore T, Wilson CH, Nicholson ML. Normothermic machine perfusion for the assessment and transplantation of declined human kidneys from donation after circulatory death donors. *Br J Surg*. 2018;105(4):388–94.
6. Heeman W, Steenbergen W, van Dam GM, Boerma EC. Clinical applications of laser speckle contrast imaging: a review. *J Biomed Opt*. 2019;24(8):1–11.
7. Feng X, Yu Y, Zou D, Jin Z, Zhou C, Liu G, et al. Functional imaging of human retina using integrated multispectral and laser speckle contrast imaging. *J Biophot*. 2022;15(2):e202100285.
8. Miller DR, Ashour R, Sullender CT, Dunn AK. Continuous blood flow visualization with laser speckle contrast imaging during neurovascular surgery. *Neurophotonics*. 2022;9(2):021908.
9. Schwartz KS, Theis EN, Bunting K, McCaughey RA, Lang JA. Laser speckle contrast imaging and laser Doppler flowmetry reproducibly assess reflex cutaneous vasoconstriction. *Microvasc Res*. 2022;142:104363.
10. Sturesson C, Milstein DMJ, Post ICJH, Maas AM, van Gulik TM. Laser speckle contrast imaging for assessment of liver microcirculation. *Microvasc Res*. 2013;87:34–40.
11. Eriksson S, Jan N, Gert L, Sturesson C. Laser speckle contrast imaging for intraoperative assessment of liver microcirculation: a clinical pilot study. *Med Dev Evid Res*. 2014;7:257–61.
12. Heeman W, Maassen H, Calon J, van Goor H, Leuvenink H, van Dam GM, et al. Real-time visualization of renal microperfusion using laser speckle contrast imaging. *J Biomed Opt*. 2021;26(5):056004. doi:10.1117/1.JBO.26.5.056004
13. Venema LH, van Leeuwen LL, Posma RA, van Goor H, Ploeg RJ, Hannaert P, et al. Impact of red blood cells on function and metabolism of porcine deceased donor kidneys during normothermic machine perfusion. *Transplantation*. 2022;106(6):1170–9.
14. Ogurlu B, Pamplona CC, Van Tricht IM, Hamelink TL, Lantinga VA, Leuvenink HGD, et al. Prolonged controlled oxygenated rewarming improves immediate tubular function and energetic recovery of porcine kidneys during normothermic machine perfusion. *Transplantation*. 2023;107(3):639–47. doi:10.1097/TP.0000000000004427
15. Boas DA, Dunn AK. Laser speckle contrast imaging in biomedical optics. *J Biomed Opt*. 2010;15(1):011109.
16. Briers D, Duncan DD, Hirst E, Kirkpatrick SJ, Larsson M, Steenbergen W, et al. Laser speckle contrast imaging: theoretical and practical limitations. *J Biomed Opt*. 2013;18(6):066018.
17. Zheng C, Lau LW, Cha J. Dual-display laparoscopic laser speckle contrast imaging for real-time surgical assistance. *Biomed Opt Express*. 2018;9(12):5962–81.
18. Gopalan C, Kirk E. Chapter 7—Renal physiology. In: Gopalan C, Kirk E, editors. *Biology of Cardiovascular and Metabolic Diseases*. Academic Press; 2022. p. 123–40.

19. Aristotle S, Sundarapandian P, Felicia C. Anatomical study of variations in the blood supply of kidneys. *J Clin Diagn Res.* 2013;7(8):1555–7.
20. Schutter R, Lantinga VA, Hamelink TL, Pool MBF, Varsseveld OC, Potze JH, et al. Magnetic resonance imaging assessment of renal flow distribution patterns during ex vivo normothermic machine perfusion in porcine and human kidneys. *Transpl Int.* 2021;34(9):1643–55.
21. Bakir N, Sluiter WJ, Ploeg RJ, van Son WJ, Tegzess AM. Primary renal graft thrombosis. *Nephrol Dial Transplant.* 1996;11(1):140–7.
22. Hurst FP, Abbott KC, Neff RT, Elster EA, Falta EM, Lentine KL, et al. Incidence, predictors and outcomes of transplant renal artery stenosis after kidney transplantation: analysis of USRDS. *Am J Nephrol.* 2009;30(5):459–67.
23. Davis MA, Kazmi SMS, Dunn AK. Imaging depth and multiple scattering in laser speckle contrast imaging. *J Biomed Opt.* 2014;19(8):086001.

SUPPORTING INFORMATION

Additional supporting information can be found online in the Supporting Information section at the end of this article.

How to cite this article: Fang Y, Ooijen van L, Ambagtsheer G, Nikolaev AV, Clahsen-van Groningen MC, Dankelman J, et al. Real-time laser speckle contrast imaging measurement during normothermic machine perfusion in pretransplant kidney assessment. *Lasers Surg Med.* 2023;1–10. <https://doi.org/10.1002/lsm.23715>